

Online Calibration of Path Loss Exponent in Wireless Sensor Networks

Guoqiang Mao^{*†‡}, Brian D.O. Anderson^{†§} and Barış Fidan^{†§}

^{*}School of Electrical and Information Engineering, the University of Sydney.

[†] Research School of Information Sciences and Engineering, Australian National University

[‡] National ICT Australia Limited[1], Sydney, Australia

[§]National ICT Australia Limited, Canberra, Australia

Abstract—The path loss exponent (PLE) is a parameter indicating the rate at which the received signal strength (RSS) decreases with distance, and its value depends on the specific propagation environment. Path loss exponent estimation plays an important role in distance-based wireless sensor network localization, where distance is estimated from the RSS measurements. Path loss exponent estimation is also useful for other purposes like sensor network dimensioning. Existing techniques on PLE estimation rely on both RSS measurements and distance measurements in the same environment to calibrate the PLE. However distance measurements can be difficult and expensive to obtain in some environments. In this paper we propose a technique for online calibration of the path loss exponent in wireless sensor networks without using distance measurements. The major contribution of this paper is to demonstrate that it is possible to estimate the PLE using only power measurements and the geometric constraints associated with planarity in a sensor network. This may have a significant impact on wireless sensor network localization.

I. INTRODUCTION

The wireless received signal strength (RSS) has been popularly modeled by a log-normal model [1], [2], [3]:

$$P_{ij}[dBm] \sim N(\overline{P_{ij}}[dBm], \sigma_{dB}^2), \quad (1)$$

$$\overline{P_{ij}}[dBm] = P_0(d_0)[dBm] - 10 \times \alpha \times \log_{10}(d_{ij}/d_0), \quad (2)$$

where $P_{ij}[dBm]$ is the received power at a receiving node j from a transmitting node i in dB milliwatts, $\overline{P_{ij}}[dBm]$ is the mean power in dB milliwatts, σ_{dB}^2 is the variance of the shadowing, $P_0(d_0)[dBm]$ is the received power in dB milliwatts at a reference distance d_0 and d_{ij} is the distance between nodes i and j . In this paper, we use the notation $[dBm]$ to denote that power is measured in dB milliwatts. Otherwise, it is measured in milliwatts. The reference power $P_0(d_0)[dBm]$ is calculated using the free space Friis equation or obtained through field measurements at distance d_0 [2]. It is important to notice that the reference distance d_0 should always be in the far field of the transmitter antenna so that the near-field effect does not alter the reference power. In large coverage cellular systems, a 1 km reference distance is commonly used, whereas in microcellular systems, a much

smaller distance such as 100 m or 1 m is used [2]. In this paper, it is assumed that d_0 and $P_0(d_0)[dBm]$ can be obtained from a *a priori* calibration of the wireless device and they are known constants. In many cases, $P_{ij}[dBm] \neq P_{ji}[dBm]$ due to the asymmetric wireless signal propagation path from node i to node j and from node j to node i . However in this paper, it is assumed that $P_{ij}[dBm] = P_{ji}[dBm]$ for simplicity. In the case of an asymmetric path, the average value of $P_{ij}[dBm]$ and $P_{ji}[dBm]$ is used. It is also assumed that all distances are normalized with respect to d_0 . Therefore Eq. 2 can be simplified as:

$$\overline{P_{ij}}[dBm] = P_0(d_0)[dBm] - 10\alpha \log_{10} d_{ij}. \quad (3)$$

The parameter α is called the path loss exponent (PLE), which indicates the rate at which the received signal strength decreases with distance. The value of α depends on the specific propagation environment. In this paper, it is assumed that α is an unknown constant, which is to be determined. For a large wireless sensor network spanning a wide area with different environmental conditions, the area can be divided into smaller regions and α can be considered as a constant in each region. Path loss exponent estimation plays an important role in distance-based wireless sensor network localization, where distance is estimated from the received signal strength measurements [4]. Path loss exponent estimation is also useful for other purposes like sensor network dimensioning. As the value of the path loss exponent depends on the environment in which a sensor network is deployed, existing techniques on path loss exponent estimation rely on both RSS measurements and distance measurements in the same environment to calibrate the path loss exponent [1], [3]. RSS measurements are readily available. However distance measurements can be difficult and expensive to obtain in some environments. Moreover, the reliance on distance measurements impedes deployment in unknown environments.

In this paper we propose a technique for online calibration of the path loss exponent in wireless sensor networks using the Cayley-Menger determinant [5], [6], which does not rely on distance measurements. The proposed technique also does not assume knowledge of the quantity σ_{dB}^2 in Eq. 1. The major contribution of this paper is to demonstrate that it is possible to estimate the PLE using only power measurements and the geometric constraints associated with planarity in a sensor

¹National ICT Australia is funded by the Australian Governments Department of Communications, Information Technology and the Arts and the Australian Research Council through the *Backing Australia's Ability initiative* and the ICT Centre of Excellence Program.

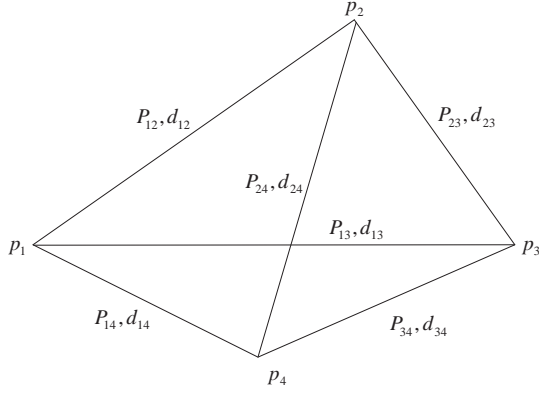


Fig. 1. A fully-connected planar quadrilateral in sensor network.

network. This may have a significant impact on distance-based wireless sensor network localization. For ease of explanation, the paper focuses on path loss exponent estimation in 2D. However the proposed technique may also be extended to 3D.

The rest of the paper is organized as follows. In Section II we present the fundamental principle underpinning the proposed technique as well as an introduction to the proposed algorithm. The presence of noise in the log-normal model means that considerable adjustment is required of an algorithm initially developed for the noiseless case, to correct for the presence of bias. In Section III, the proposed algorithm is validated using both simulations and real measurement data. Conclusions and suggestions to further work are given in Section IV.

II. PATH LOSS EXPONENT ESTIMATION BASED ON THE CAYLEY-MENGER DETERMINANT

Consider a sensor with three neighbors where the neighbors of that sensor are also neighbors of each other. Two sensors i and j are neighbors if P_{ij} is nonzero. The sensor and its neighbors can be represented by a full-connected planar quadrilateral shown in Fig. 1. The tuple (P_{ij}, d_{ij}) represents the measured power and the true distance between node i and node j respectively. P_{ij} and d_{ij} are related through Eq. 1 and Eq. 3. The path loss exponent estimation problem can be formulated as the simultaneous estimation of the true distances $d_{12}, d_{13}, d_{14}, d_{23}, d_{24}, d_{34}$ and α given the power measurements $P_{12}, P_{13}, P_{14}, P_{23}, P_{24}, P_{34}$. Using the maximum likelihood estimator, the likelihood function can be obtained as:

$$L(d_{12}, d_{13}, d_{14}, d_{23}, d_{24}, d_{34}, \alpha) = \frac{1}{(\sqrt{2\pi}\sigma_{dB})^6} \times \prod_{1 \leq i < j \leq 4} \exp\left(-\frac{(P_{ij}[dBm] - P_0(d_0)[dBm] + 10\alpha \log_{10} d_{ij})^2}{\sigma_{dB}^2}\right)$$

As the number of power measurements is smaller than the number of parameters to be estimated, this leads to a set of simple equations. In these equations P_{ij} and $P_0(d_0)$ are in

decimal units, not in dB units, so that $P_{ij} = 10^{P_{ij}[dBm]/10}$.

$$P_{12} = P_0(d_0) \times d_{12}^{-\alpha} \quad (4)$$

$$P_{13} = P_0(d_0) \times d_{13}^{-\alpha} \quad (5)$$

$$P_{14} = P_0(d_0) \times d_{14}^{-\alpha} \quad (6)$$

$$P_{23} = P_0(d_0) \times d_{23}^{-\alpha} \quad (7)$$

$$P_{24} = P_0(d_0) \times d_{24}^{-\alpha} \quad (8)$$

$$P_{34} = P_0(d_0) \times d_{34}^{-\alpha} \quad (9)$$

Another constraint that is required to solve the above equations can be found from the geometric constraint on a fully-connected planar quadrilateral using the Cayley-Menger determinant [5], [6]. The Cayley-Menger determinant of a quadrilateral is given by:

$$D(p_1, p_2, p_3, p_4) = \begin{vmatrix} 0 & d_{12}^2 & d_{13}^2 & d_{14}^2 & 1 \\ d_{12}^2 & 0 & d_{23}^2 & d_{24}^2 & 1 \\ d_{13}^2 & d_{23}^2 & 0 & d_{34}^2 & 1 \\ d_{14}^2 & d_{24}^2 & d_{34}^2 & 0 & 1 \\ 1 & 1 & 1 & 1 & 0 \end{vmatrix} \quad (10)$$

A classical result on the Cayley-Menger determinant is given by the following theorem:

Theorem 1: (Theorem 112.1 in [6]) Consider an n -tuple of points p_1, \dots, p_n in m -dimensional space with $n \geq m + 1$. The rank of the Cayley-Menger matrix $M(p_1, \dots, p_n)$ (defined analogously to the right side of Eq. 10 but without the determinant operation) is at most $m + 1$.

A direct application of the theorem leads to:

$$D(p_1, p_2, p_3, p_4) = 0. \quad (11)$$

Combining Eq. 11 and Eq. 4 to Eq. 9, a nonlinear equation for α can be obtained:

$$h(\alpha) = \begin{vmatrix} 0 & C_{12}^{-2/\alpha} & C_{13}^{-2/\alpha} & C_{14}^{-2/\alpha} & 1 \\ C_{12}^{-2/\alpha} & 0 & C_{23}^{-2/\alpha} & C_{24}^{-2/\alpha} & 1 \\ C_{13}^{-2/\alpha} & C_{23}^{-2/\alpha} & 0 & C_{34}^{-2/\alpha} & 1 \\ C_{14}^{-2/\alpha} & C_{24}^{-2/\alpha} & C_{34}^{-2/\alpha} & 0 & 1 \\ 1 & 1 & 1 & 1 & 0 \end{vmatrix} = 0, \quad (12)$$

where $C_{ij} = P_{ij}/P_0(d_0)$, $1 \leq i < j \leq 4$, and the C_{ij} are all known. An analytical solution to Eq. 12 is difficult to find. However Eq. 12 can be conveniently solved using the bracketing and bisection numerical technique [7, section 9.1].

Unfortunately, the estimate of α obtained using this method shows a strong bias, i.e.,

$$B_{\hat{\alpha}} = E(\hat{\alpha}) - \alpha. \quad (13)$$

Fig. 2 shows a histogram of the estimated path loss exponent, which is obtained from simulation using 10,000 different quadrilaterals whose vertices are uniformly distributed in a square region of 15×15 . Other parameters used in the simulation are: the true value of α is 2.3; $\sigma_{dB} = 3.92$; $P_0(d_0)[dBm] = -37.4603dBm$; $d_0 = 1m$. These parameters are drawn from real measurement data reported in [1]. It should be noted that in the presence of noise in power measurements, Eq. 12 may have non-unique solutions even in the typical range of α

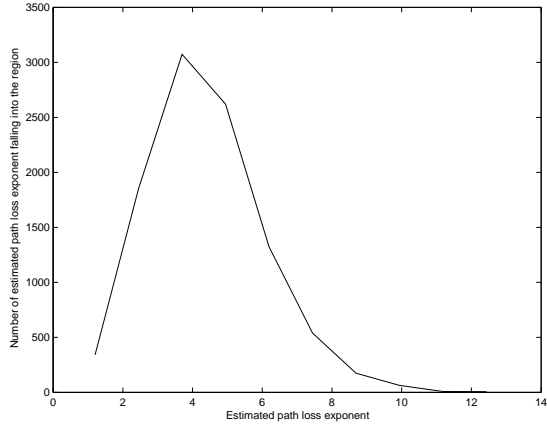


Fig. 2. Histogram of the estimated path loss exponent using Cayley-Menger determinant. The figure is obtained using 10,000 quadrilaterals whose vertices are uniformly distributed in a square region of 15×15 .

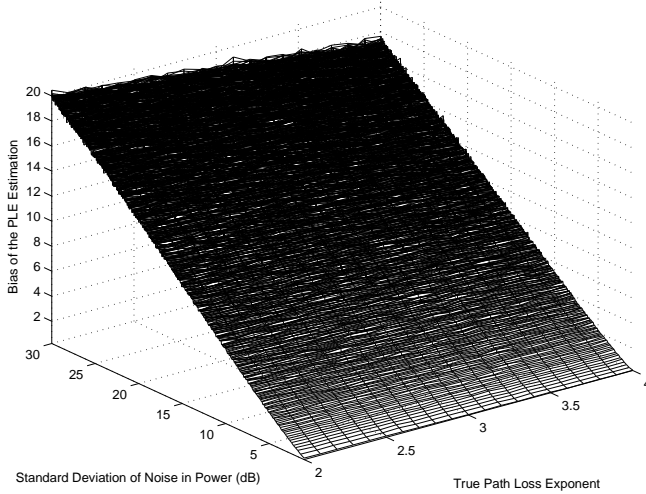


Fig. 3. Relationship between the bias of $\hat{\alpha}$, the standard deviation of noise in power measurement σ_{dB} and α . $B_{\hat{\alpha}}$ depends to a small degree on α as well as on σ_{dB}^2 .

for some quadrilaterals. In that case, we simply discard that quadrilateral and do not use it in the calculation to avoid any ambiguity. As shown in the figure, the true value of α is 2.3 and the estimated value of α has a bias of 2.08. The simulation shows that $\hat{\alpha}$ obtained using the aforementioned technique has a strong bias which cannot be ignored.

Bias removal requires an analysis on $E(\hat{\alpha})$. However a direct analysis of $E(\hat{\alpha})$ is difficult because of the difficulty in obtaining an explicit analytical expression of α from Eq. 12. Therefore we resort to numerical experiments to evaluate $E(\hat{\alpha})$. Our numerical evaluation shows that the bias of $\hat{\alpha}$, $B_{\hat{\alpha}}$, has an approximate linear relationship with σ_{dB} for a fixed α . This is shown in Fig. 3. Fig. 3 is obtained using 3,000 quadrilaterals whose vertices are uniformly distributed in a square of 15×15 . The corresponding power measurements are obtained using Eq. 1 and Eq. 3.

Moreover further simulations show that the relationship be-

tween $B_{\hat{\alpha}}$, σ_{dB} and α is almost independent of the distribution of the vertices of the quadrilaterals and is also independent of the shape of the area in which the vertices of the quadrilaterals are located. As an example, Fig. 4 shows the relationship between $B_{\hat{\alpha}}$ and σ_{dB} for quadrilaterals whose vertices are located in areas of a variety of different shapes and distributed in the area following different distributions. Fig. 5 shows the relationship between $B_{\hat{\alpha}}$ and σ_{dB} at a specific value of $\alpha = 2.3$.

Based on the observation shown in Fig. 4 and Fig. 5 that the relationship between $B_{\hat{\alpha}}$ and σ_{dB} is independent of the distribution of the vertices of various quadrilaterals and the shape of the area in which vertices of the quadrilaterals are located, a pattern matching technique can be used to estimate the path loss exponent which uses the power measurements only.

Specifically, via *a priori* simulation, a data base can be established where each entry in the data base is arranged in the form $(\alpha_i, \sigma_{dB,j}^2, E(\hat{\alpha})_{\alpha_i, \sigma_{dB,j}^2})$. The symbol $E(\hat{\alpha})_{\alpha_i, \sigma_{dB,j}^2}$ is used to emphasize dependence of $E(\hat{\alpha})$ on the path loss exponent α_i and the variance of noise in power measurements $\sigma_{dB,j}^2$. This data base can be obtained using a large number of quadrilaterals whose vertices, say, are uniformly distributed in an area. The corresponding power measurements are obtained using Eq. 1 and Eq. 3. The distance between adjacent σ_{dB}^2 is the same, i.e.,

$$\sigma_{dB,j+1}^2 - \sigma_{dB,j}^2 = \Delta\sigma_{dB}^2. \quad (14)$$

The distance between adjacent α is also the same, i.e.,

$$\alpha_{i+1} - \alpha_i = \Delta\alpha. \quad (15)$$

Given this data base, the estimation of α can be obtained using the following procedure for pattern matching:

- 1) Identify a set of fully connected quadrilaterals in the wireless sensor network for further computation;
- 2) Add a random Gaussian noise with variance $\Delta\sigma_{dB}^2$ into each power measurement. The power is measured in dB milliwatts unit;
- 3) For each individual quadrilateral, solve for $\hat{\alpha}$ using Eq. 12. An $E(\hat{\alpha})_{r,1}$ corresponding to $\Delta\sigma_{dB}^2$ can be obtained as the average value of $\hat{\alpha}$ obtained from each individual quadrilateral. Here the subscript r is used to mark the difference with the corresponding value in the database;
- 4) Repeat steps 2 and 3 using different noise variance values $M\Delta\sigma_{dB}^2$, where $M = 0, 1, 2, \dots, m$. Here $M = 0$ corresponds to the original data set without the additionally introduced noise. A series of tuples $(0, E(\hat{\alpha})_{r,0}), (\Delta\sigma_{dB}^2, E(\hat{\alpha})_{r,1}), \dots, (m\Delta\sigma_{dB}^2, E(\hat{\alpha})_{r,m})$ can then be obtained;
- 5) Search the database and find the values of i and j such that:

$$\{i, j\} = \underset{N=0}{\operatorname{argmin}} \sum_{N=0}^m (E(\hat{\alpha})_{r,N} - E(\hat{\alpha})_{\alpha_i, \sigma_{dB,j+N}^2})^2. \quad (16)$$

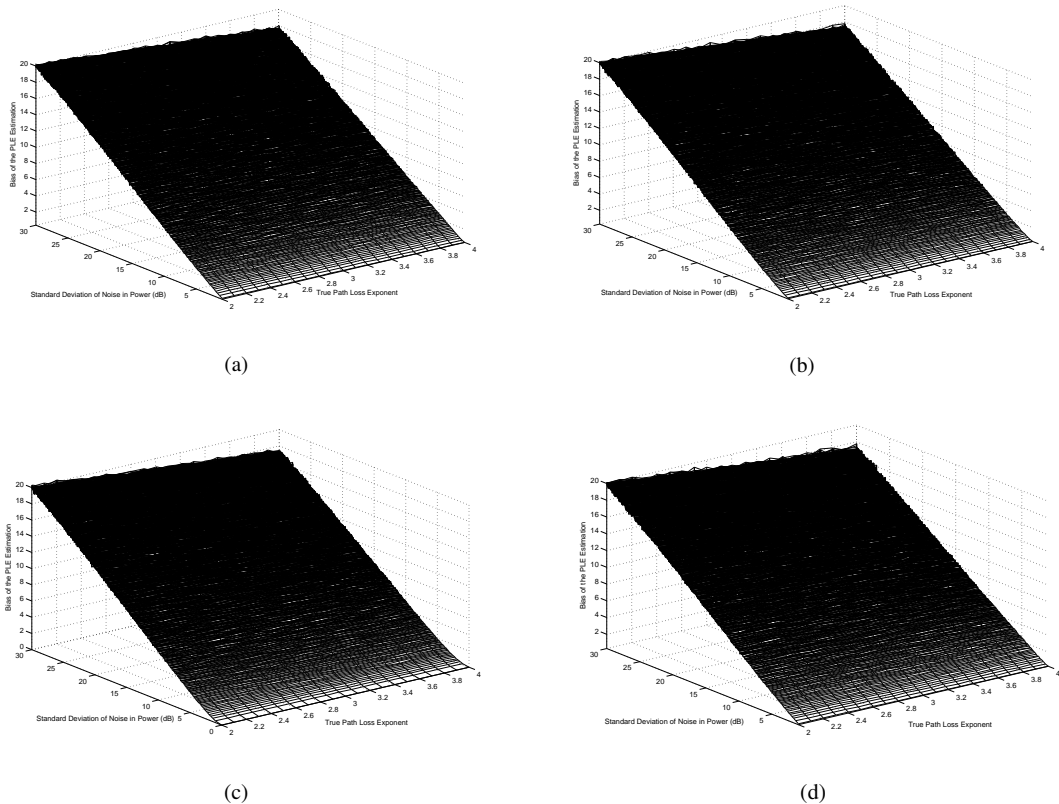


Fig. 4. Relationship between the bias of $\hat{\alpha}$ and the standard deviation of noise in power measurement σ_{dB} . The relationship between $B_{\hat{\alpha}}$ and σ_{dB} is almost independent of the distribution of the vertices of the quadrilaterals and independent of the shape of the area in which the vertices of the quadrilaterals are located. a) Generated from 3000 quadrilaterals whose vertices are uniformly distributed in a “L” shaped area. b) Generated from 3000 quadrilaterals whose vertices are uniformly distributed in a rectangular area of 10×20 . c) Generated from 3000 quadrilaterals whose vertices are distributed in a square area of 15×15 following a truncated Gaussian distribution with a zero mean and a standard variation of 5. d) Generated from 3000 quadrilaterals whose vertices are located in a ring. The inner radius of the ring is 5 and the outer radius is 10. The coordinates of the vertices are generated by first selecting a number uniformly distributed in $[5, 10]$ and then selecting a number uniformly distributed in $[0, 2\pi]$. The two numbers are used as the polar coordinate of the vertex to obtain the rectangular coordinate.

The parameter m has to be a large number, say ≥ 500 , in order to obtain a reasonably accurate estimate of α , which is robust against the randomness in the data.

- 6) Finally, an improved estimate of α approximately correcting for the bias can be obtained as:

$$\hat{\alpha} = \alpha_i. \quad (17)$$

Similarly, an estimate of σ_{dB} can be obtained as:

$$\hat{\sigma}_{dB} = \sigma_{dB,j}. \quad (18)$$

III. SIMULATION VALIDATION

In this section, we shall validate the proposed technique using both simulations and real measurements. The database is established by simulations using 3,000 quadrilaterals whose vertices are uniformly distributed in a square region of 15×15 . The measured power is generated using Eq. 1 and Eq. 3. $\Delta\sigma_{dB}^2$ is set to be 1 and the distance between adjacent α_i is set to be 0.1, i.e., $\Delta\alpha = 0.1$. Another set of 3,000 quadrilaterals whose vertices is uniformly distributed in a rectangular area of 10×20 are used to establish the performance of the proposed algorithm. 700 points are used in the search, i.e., $m = 700$

in Eq. 16. The simulation is repeated by varying the value of α from 2 to 4 and varying the value of σ_{dB} from 5 to 10, which are the typical ranges of the two parameters [2]. Fig. 6 shows the error in estimating α and Fig. 7 shows the error in estimating σ .

As shown in Fig. 6, the error in estimating α is contained in the region $[-0.3, 0.1]$. The mean estimation error is -0.1175 and the error variance is 0.0115. Fig. 7 shows that the error in estimating σ_{dB} is contained in the region $[0, 1]$. The mean estimation error is 0.4827 and the error variance is 0.0263. Fig. 7 also shows that the error in estimating σ_{dB} is larger at smaller values of σ_{dB} . This is attributable to the larger separation between $\sigma_{dB,j+1}$ and $\sigma_{dB,j}$ at smaller values of $\sigma_{dB,j}$. The impact of the estimation error depends on the specific application, density of sensor network and deployment of sensors. It is beyond the scope of this paper to evaluate the impact of the estimation error.

The estimation error is attributable to the randomness in the data and can be reduced by using smaller values of $\Delta\sigma_{dB}^2$ and $\Delta\alpha$ at the expense of increased computational load. For example, our simulation (not shown here due to space limitation) shows that by using $m = 2800$, $\Delta\alpha = 0.05$ and

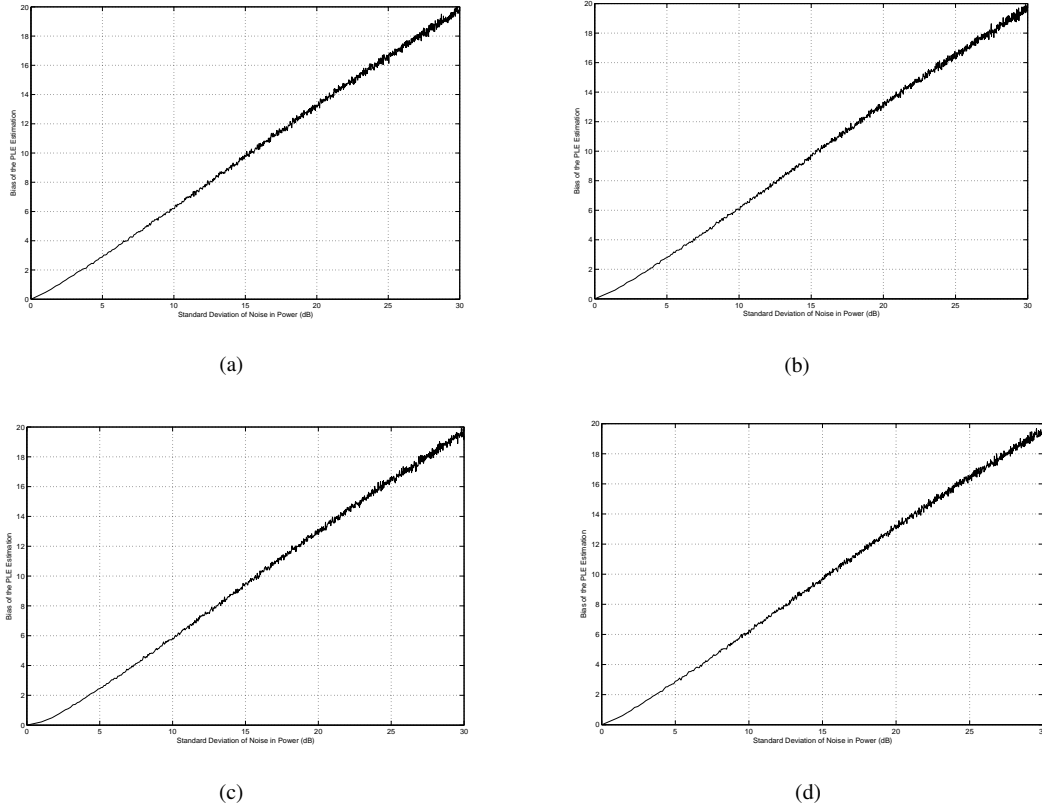


Fig. 5. Relationship between the bias of $\hat{\alpha}$ and the standard deviation of noise in power measurement σ_{dB} at a specific value of α . Subfigures a), b), c), d) are obtained under the same conditions as those in Fig. 4.

$\Delta\sigma_{dB}^2 = 0.25$, the maximum error in estimating α reduces to 0.2. The mean error reduces to -0.0603 and the error variance reduces to 0.0056. Another possible approach to reducing estimation error is by applying a noise reduction technique [8] to data before the pattern matching.

Simulations using quadrilaterals whose vertices are distributed in an area of a different shape and/or following a different distribution show similar performance. Fig. 8 and Fig. 9 show the simulation results using a set of 3,000 quadrilaterals whose vertices are distributed in a square region of 15×15 following a truncated two-dimensional Gaussian distribution. The mean of the Gaussian distribution is at the center of the square region and the standard deviation of the Gaussian distribution is 5. Both figures show similar performance as those in Fig. 6 and Fig. 7 except that the estimation error of α has a value of -0.4 at a couple of points in Fig. 8. However the estimation error of σ_{dB} is better than that in Fig. 7.

To further evaluate the performance of the proposed technique, we apply it to real measurement data reported in [1]. The measurement data and the deployment of sensors can also be found at <http://www.eecs.umich.edu/~hero/localize/>. The wireless sensor network in [1] consists of 44 fully connected nodes, which make up 135,751 quadrilaterals. It is both computationally intensive and unnecessary to compute $\hat{\alpha}$ for each quadrilateral. Here we randomly choose 10,000 quadri-

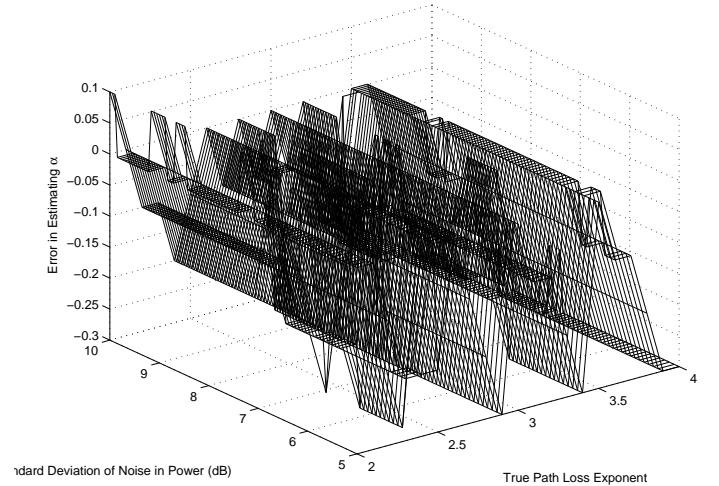


Fig. 6. Error in estimating α using the pattern matching. The vertices of the quadrilaterals are uniformly distributed in a rectangular area of 10×20 .

laterals for computation. The reference power $P_0(d_0)[dBm]$ is calculated using the free space Friis equation at a reference distance $d_0 = 1m$ and $P_0(d_0)[dBm] = -37.4663dBm$ [1]. The path loss exponent estimated using both the power measurements and the measured distances is 2.3022. The path loss exponent estimated using the proposed technique is 2.2, which represents an error of -0.1022 . The true value σ_{dB}

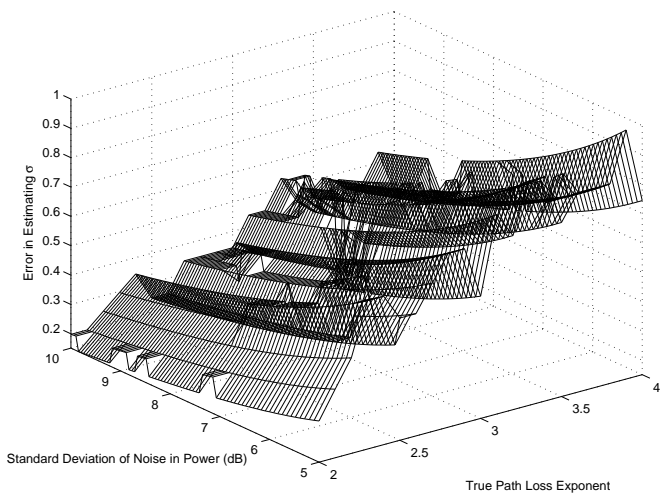


Fig. 7. Error in estimating σ_{dB} using the pattern matching. The vertices of the quadrilaterals are uniformly distributed in a rectangular area of 10×20 .

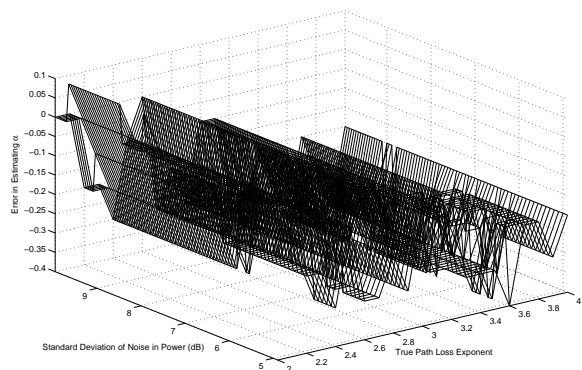


Fig. 8. Error in estimating α using the pattern matching. The vertices of the quadrilaterals are distributed in a square region of 15×15 following a truncated two-dimensional Gaussian distribution.

(i.e., the value obtained using real power measurements and measured distances) is 3.92 and the estimation error is -1.50 . The slightly larger error in estimating σ_{dB} when using real measurement data may be attributable to the density of the noise in the power measurements deviating from a Gaussian distribution.

IV. CONCLUSION AND FURTHER WORK

In this paper, we proposed an algorithm which can estimate the path loss exponent using only power measurements and the underlying planar geometric constraints on the sensors only. The algorithm is based on the Cayley-Menger determinant and it does not use any distance measurements. The algorithm is validated using both simulations and real measurement data.

The proposed algorithm may have significant impact on distance-based wireless sensor network localization. In this paper, we observed the empirical law that the relationship between $B_{\hat{\alpha}}$, σ_{dB} and α is independent of the distribution of the vertices of the quadrilaterals and is also independent of

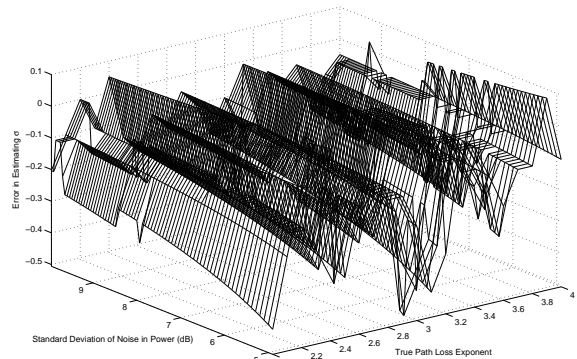


Fig. 9. Error in estimating σ_{dB} using the pattern matching. The vertices of the quadrilaterals are distributed in a square region of 15×15 following a truncated two-dimensional Gaussian distribution.

the shape of the area in which the vertices of the quadrilaterals are located. It is desirable to obtain an analytical expression of the relationship between $B_{\hat{\alpha}}$, σ_{dB} and α . This is also the direction of our future research.

Furthermore, the proposed algorithm relies on the log-normal propagation model in Eq. 1 and Eq. 2 in the sense that the maximum likelihood estimator shown in Eq. 4 to Eq. 9 may have a different form when the received signal strength has a different model. Although the log-normal propagation model is a popular model for wireless network, there are environments in which the log-normal propagation model is not the best model [2]. In that case, a technique needs to be developed to select the best model and choose the best estimator for distance to replace Eq. 4 to Eq. 9 accordingly. Therefore how to develop an algorithm for environments in which the log-normal propagation model does not apply is also a future research topic.

REFERENCES

- [1] N. Patwari, I. Hero, A.O., M. Perkins, N. Correal, and R. O'Dea, "Relative location estimation in wireless sensor networks," *IEEE Transactions on Signal Processing*, vol. 51, no. 8, pp. 2137–2148, 2003.
- [2] T. S. Rappaport, *Wireless Communications: Principles and Practice*, 2nd ed. Prentice Hall PTR, 2001.
- [3] D. Lymberopoulos, Q. Lindsey, and A. Savvides, "An empirical analysis of radio signal strength variability in IEEE 802.15.4 networks using monopole antennas, Tech. Rep. ENALAB Technical Report 050501, 2005.
- [4] G. Mao, B. Fidan, and B. D. O. Anderson, "Sensor network localization," in *Sensor Network and Configuration: Fundamentals, Techniques, Platforms and Experiments*. Germany: Springer-Verlag, 2006.
- [5] G. M. Crippen and T. F. Havel, *Distance Geometry and Molecular Conformation*. New York: John Wiley and Sons Inc., 1988.
- [6] L. M. Blumenthal, *Theory and Applications Distance Geometry*. Oxford University Press, 1953.
- [7] W. H. Press, S. A. Teukolsky, W. T. Vetterling, and B. P. Flannery, *Numerical Recipes in C - The Art of Scientific Computing*, 2nd ed. Cambridge University Press, 2002.
- [8] S. V. Vaseghi, *Advanced Digital Signal Processing and Noise Reduction*, 3rd ed. John Wiley & Sons, 2006.